Human Pathology (2009) 40, 1278–1287

ELSEVIER

Human
PATHOLOGY

www.elsevier.com/locate/humpath

Original contribution

The definition of fibrogenic processes in fibroblastic foci of idiopathic pulmonary fibrosis based on morphometric quantification of extracellular matrices

Masahiro Yamashita MD[a,*], Kohei Yamauchi MD[b], Ryoji Chiba MD[c], Noriyuki Iwama MD[c], Fumiko Date[a], Naoko Shibata[a], Hiroyuki Kumagai MD[a], Juha Risteli MD[d], Shinobu Sato MD[e], Tohru Takahashi MD[f], Masao Ono MD[a]

[a]*Department of Pathology, Tohoku University Graduate School of Medicine, Sendai, Miyagi 980-8575, Japan*
[b]*Department of Respiratory Medicine, Iwate Medical University, Morioka, Iwate 020-8505, Japan*
[c]*Department of Pathology, Sendai Kosei Hospital, Sendai, Miyagi, Japan*
[d]*Department of Clinical Chemistry, Oulu University, Oulu, Finland*
[e]*Department of Internal Medicine, Saka General Hospital, Shiogama, Miyagi 985-8506, Japan*
[f]*Department of Pathology, Ishinomaki Red Cross Hospital, Ishinomaki, Miyagi 980-8522, Japan*

Received 4 November 2008; revised 27 January 2009; accepted 30 January 2009

Keywords:
Fibroblastic foci;
Extracellular matrix;
Matrix metalloproteinase;
Capillary angiogenesis;
Lymphangiogenesis

Summary There is limited information regarding the process of tissue remodeling in fibroblastic foci associated with idiopathic pulmonary fibrosis. The aim of this study was to identify the different pathologic stages of tissue remodeling in fibroblastic foci based on the histopathologic differences in the glycosaminoglycan distribution and collagen deposition. In addition, we also aimed at clarifying the stage-specific characteristics by taking into consideration the expression pattern of matrix metalloproteinase and angiogenesis. Lung biopsies of 16 patients with idiopathic pulmonary fibrosis were used. The presence of glycosaminoglycans was detected by Alcian blue staining, and type I collagen was detected by immunohistochemical analysis with a primary antibody specific to the cross-linked carboxyterminal telopeptide of type I collagen. The fibroblastic foci characterized by the expression intensity of Alcian blue and telopeptide of type I collagen were divided into 3 groups, namely, Alcian blue^{+}telopeptide of type I collagen^{weak}, Alcian blue^{+}telopeptide of type I collagen^{+}, and Alcian blue^{weak}telopeptide of type I collagen^{+}; consequently, 3 new stages were defined—stages I, II, and III, respectively. A significant inverse correlation was observed between the area densities of Alcian blue^{+} and telopeptide of type I collagen^{+} in fibroblastic foci. Stage I was characterized by the expression of matrix metalloproteinase-2 and tissue inhibitor of matrix metalloprotease-2 in fibroblasts and the overlying epithelium of fibroblastic foci, and also the absence of capillary angiogenesis. In contrast, the expression of these proteins was attenuated in stage III, except for that of matrix metalloproteinase-2 in fibroblasts. In stages II and III, capillary angiogenesis was observed. Lymphangiogenesis was

* Corresponding author.
E-mail address: yamam@mail.tains.tohoku.ac.jp (M. Yamashita).

doi:10.1016/j.humpath.2009.01.014

undetected in all the 3 stages. Thus, pathologic staging helps understand the roles of the factors involved in tissue remodeling in idiopathic pulmonary fibrosis.

1. Introduction

Idiopathic pulmonary fibrosis (IPF) is a chronic and progressive fibrogenic disease of unknown etiology, and it is believed to be a consequence of aberrant healing of a lung injury [1]. IPF is histologically characterized by chronic interstitial pneumonia, small aggregates of myofibroblasts and fibroblasts (termed as fibroblastic foci [FF]), and dense collagen and honeycomb change [2]. FF consist of an extracellular matrix (ECM), overlying epithelium, and a small aggregate of fibroblasts expressing procollagen proteins [2]. It has been considered that FF represent a leading edge of fibrogenesis during the development of IPF [3-7], although the prognostic significance of FF in IPF patients is still controversial [8-10].

A variety of factors that are involved in tissue remodeling of IPF have been examined. The synthesis/degradation of the ECM in FF, in which collagen, cell adhesion protein, and proteoglycans (PGs) are present [11-15], has been of particular interest in this pathologic condition. Matrix metalloproteinase-2 (MMP-2) is a regulator of matrix degradation, and tissue inhibitor of matrix metalloproteinase (TIMP-2) inhibits the activity of MMP-2 by binding to pro-MMP-2. The expression of MMP-2 and TIMP-2 has been observed in fibroblasts and in the overlying epithelium of FF. It has been suggested that these factors play a role in the excessive collagen deposition in the ECM [16-23]. It has also been shown that capillary angiogenesis is involved in tissue remodeling in pulmonary fibrosis [24-29]. In particular, in the case of IPF, $CD34^+$ capillaries are barely detectable in FF [28,29]. It has been speculated that the absence of capillary angiogenesis in FF leads to the poor prognosis of IPF.

There is limited information regarding the fibrogenic processes occurring in FF during the development of IPF. It has been reported that versican—a type of PG that consists of a core protein linked to glycosaminoglycans (GAGs)—is observed in FF and that mature collagen is barely detected in versican-rich lesions [30]. This report suggests that multiple temporal phases may be recognizable in the matrix turnover of FF. In the present study, we performed the pathologic staging of FF by characterizing GAG distribution and collagen deposition in FF. Based on the staging, we investigated the expression patterns of MMP-2 and TIMP-2 and the occurrence of capillary angiogenesis and lymphangiogenesis in FF. In a recent study, lymphangiogenesis has been shown to occur in fibrogenic conditions [31-33]. The pathologic staging of FF provides a deeper understanding of tissue remodeling that occurs during IPF.

2. Materials and methods

2.1. Materials

All lung specimens were obtained by surgical biopsies from 16 patients with IPF, which was diagnosed based on American Thoracic Society/European Respiratory Society criteria [34] and were embedded in paraffin in the Department of Pathology of Iwate Medical University (Morioka, Japan), Ishinomaki Red Cross Hospital (Ishinomaki, Miyagi, Japan), and Saka General Hospital (Shiogama, Miyagi, Japan). Surgical biopsies were required to define the diagnoses of usual interstitial pneumonia. None had any evidence of systemic infection, iatrogenic causes of immunosuppressive agents, toxic exposures, cancer undergoing cytotoxic chemotherapy, preexisting collagen vascular diseases, or cardiac failure. No patient in an accelerated phase of interstitial pneumonia was included. The mean age of patients was 63.3 ± 7.6 (range, 50-78; male:female ratio = 10:6). Normal lung tissues were obtained from 4 patients who died independently of pulmonary diseases. Informed consent was obtained from every patient. The use of all surgical biopsy samples in the present study was approved by the ethical committees of Iwate Medical University, Ishinomaki Red Cross Hospital, and Saka General Hospital.

2.2. Histochemical and immunohistochemical examination

Alcian blue (Al-B) staining was used for the detection of GAGs as previously reported [14,15]. In brief, dewaxed sections were immersed in 100% ethanol for 10 minutes, rinsed in water for 10 minutes, immersed in 3% acetic acid for 2 minutes, and stained in 1% Alcian blue 8GS in 3% acetic acid (pH 2.5) for 1 hour. Nonspecific stain was removed with 3% acetic acid and rinsed in water for 10 minutes. Primary antibodies used in our immunohistochemical analyses are summarized in Table 1. Rabbit polyclonal antibodies to the cross-linked carboxyterminal telopeptide of type I collagen (ICTP) [35] was mainly used as the marker of mature type I collagen. A rat polyclonal antibody to the carboxyterminal propeptide of type I procollagen (PICP) was used for the detection of procollagen protein. The rabbit polyclonal antibody to MMP-2 is known to identify inactive and active forms. CD34 and D2-40 were used as the markers of capillaries and lymphatics, respectively. Deparaffinized tissue sections on glass slides were treated by blocking with 10% normal rabbit or goat serum in phosphate-buffered saline for 15 minutes at room temperature. After rinsing the slides in phosphate-buffered

Table 1 Details of primary antibodies used

Primary Antibody	Source	Isotype	Antigen retrieval methods	Concentration (μg/mL)
PICP (Millipore Corporation, Beillerica, MA)	Rat	IgG_1	AC	0.03
Type I collagen (Abcam, Cambridge, UK)	Mice	IgG_1	AC	×600 [a]
ICTP (from Dr Risteli)	rabbit	polyclonal	MW	0.1
MMP-2 (Millipore Corporation)	Rabbit	Polyclonal	none	1.7
TIMP-2 (Millipore Corporation)	Rabbit	polyclonal	none	10
α-smooth muscle actin (Dako Japan, Tokyo, Japan)	Mice	IgG_{2a} κ	none	×100 [a]
CD34 (Nichirei, Tokyo, Japan)	Mice	IgG_1	MW	0.1
D2-40 (Nichirei)	Mice	IgG_1	MW	0.26

MW, microwave irradiation for 2 minutes at 1000 W in the citrate buffer (pH 6.0); AC, autoclave for 5 minutes at 121°C.
[a] Indicates the dilution.

saline, they were incubated overnight with primary antibodies at 4°C. The antigen-antibody reaction was visualized by 3,3′-diaminobenzidine tetrahydrochloride. The sections were counterstained using resorcin-fuchsin and hematoxylin. As a reference for background staining, murine isotype-matched, nonspecific monoclonal IgG1 or normal rabbit serum was used.

Dual immunohistochemical staining using CD34 and D2-40 was performed as described previously [31]. Antigen-antibody reactions were visualized by using Vector Red (Vector Laboratories, Burlingame, CA) and diaminobenzidine tetrahydrochloride.

2.3. Morphometry analyses

The area densities of the Al-B^+ stain and the $ICTP^+$ expression contained in FF, namely, A_A(Al-B) and A_A(ICTP), and the number density of the $CD34^+$ capillary, namely, N_A(cap), were estimated in relation to FF from each section [36].

To quantitatively estimate the change in ECM remodeling in FF, we used volume density: V_v(Al-B), which is the total volume of the Al-B^+ stain in a unit volume. V_V(Al-B) was estimated with the aid of a basic principle of stereology [36]:

$$V_V(\text{Al–B}) = A_A(\text{Al–B}) \quad (1)$$

Here, A_A(Al-B) is area density defined as the fraction of the Al-B^+ staining area contained in the whole area of a fibroblastic focus. Moreover, A_A(ICTP) was also estimated. The sections stained by Al-B or immunostained by the antibody against ICTP were magnified by a charged coupled device (CCD) camera (Motic Images Plus 2.0S image analysis system; Shimazu, Kyoto, Japan), and the profiles were measured by adopting the point-counting method using a grid of 2-μm of intervals.

The degree to which capillaries developed in the lung tissue was quantified in terms of their length density in space: L_V(cap), which is the total length of the capillaries in a unit volume. This was estimated by resorting to a basic principle of stereology [36]:

$$L_V(\text{cap}) = 2N_A(\text{cap}) \quad (2)$$

Here, N_A(cap) is the numerical density of capillaries in terms of area or the number of capillaries in a unit area. In the present study, N_A(cap) was estimated as the number density of capillaries in 100-μm^2 area of a fibroblastic focus. The area of FF was measured using a digitizer, and the number of capillaries contained in FF was counted using an ocular microscope.

2.4. Statistical analysis

The relationship between the area densities of Al-B^+ and $ICTP^+$ and the relationship between the area density of ICTP and the capillary number density were evaluated using the Spearman rank correlation coefficient. A P value of less than .05 was considered as statistically significant.

3. Results

3.1. Characterization of FF by Alcian blue staining and immunostaining with carboxyterminal telopeptide of type I collagen

We characterized FF with Al-B staining and immunostaining using primary antibodies against PICP, type I collagen, and ICTP. The FF were characterized as having 3 patterns. The first set of serial sections showed an Al-B-dominant pattern. The whole ECM of a fibroblastic focus was strongly stained with Al-B (Fig. 1A), whereas immunostaining revealed low expression levels of type I collagen and ICTP (Fig. 1B, C). The expression of PICP was found to be consistent in fibroblasts of the focus (Fig. 1D). The second set of serial sections showed a mixed pattern of Al-B staining and collagen markers: Al-B stained the inner side of a fibroblastic focus, whereas the expression of type I collagen, and ICTP was noted in the peripheral regions where Al-B staining was not detected (Fig. 2A-C). The third set of serial sections showed a collagen-dominant pattern. The expression of type I collagen and ICTP was detected in the whole ECM of a fibroblastic focus, whereas weak staining was observed with Al-B (Fig. 3A-C). FF

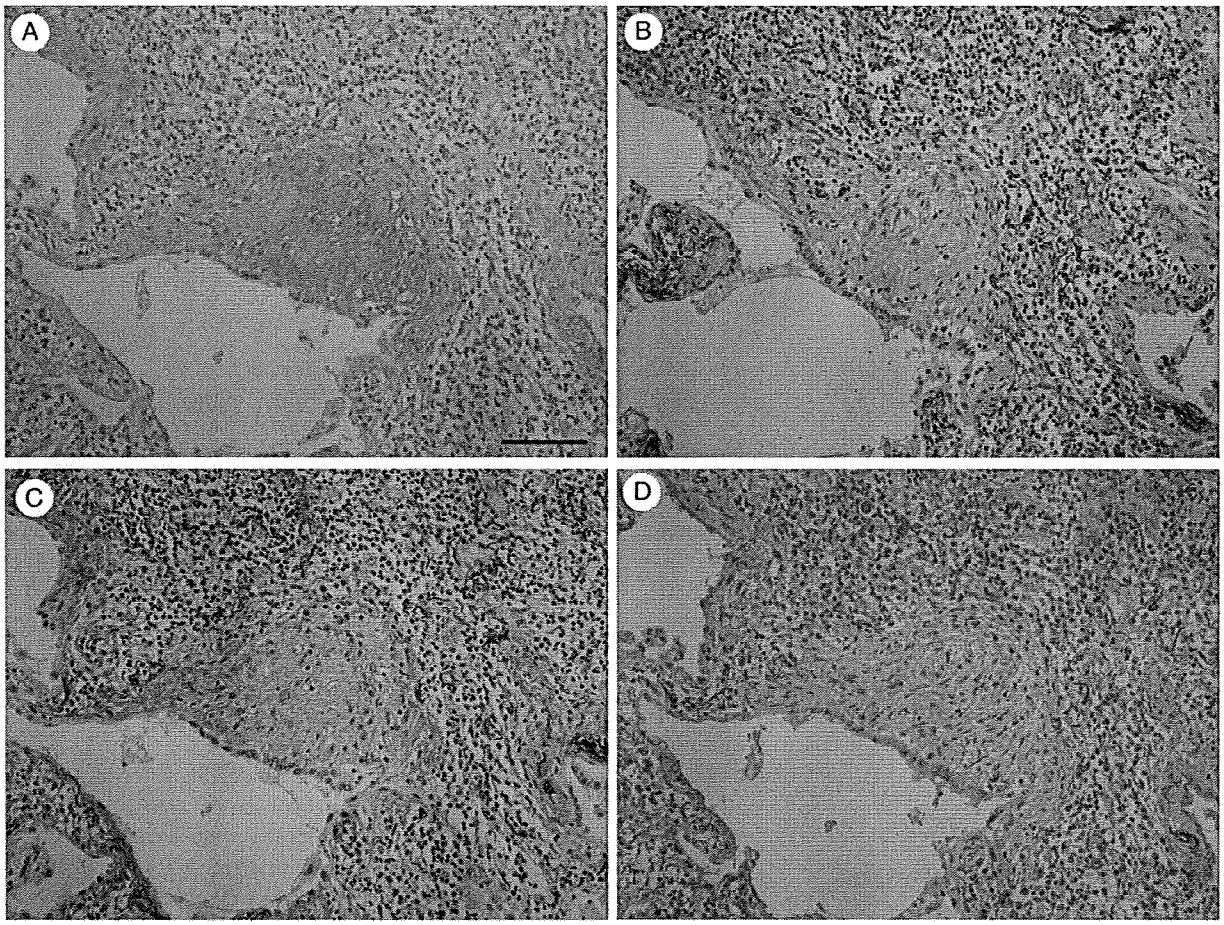

Fig. 1 An Al-B–dominant pattern of fibroblastic foci. The first set of serial sections shows that Al-B strongly stains in the whole ECM of a fibroblastic focus (A), whereas the expression of type I collagen (B) and ICTP (C) is barely observed in the focus. D, The expression of PICP is observed in fibroblasts of the focus. Hematoxylin (A-D) and Resorcin-fuchsin (B-D) for counterstain. Scale bar represents 100 μm.

exhibiting this pattern typically had a low expression of PICP in the fibroblasts, although high PICP expression was occasionally observed (Fig. 3D). The distribution of ICTP expression was found to be similar to that of mature type I collagen for all 3 staining patterns. Compared with immunostaining with antibodies against type I collagen, immunostaining with antibodies against ICTP showed less architectural deviation with regard to antigen retrieval; therefore, in the present study, we used ICTP as the marker for deposition of type I collagen. No specific trend was observed in any of the 3 aforementioned patterns with respect to the expression of α–smooth muscle actin in the fibroblasts (data not shown).

3.2. A negative correlation between Al-B+ and ICTP+ area densities in FF and the staging of FF

The area densities of Al-B$^+$ and ICTP$^+$ in FF were measured. The results demonstrated that a significantly negative correlation existed between A_A(Al-B) and A_A(ICTP) ($r = -0.832$, $P < .001$) (Fig. 4). It has been previously reported that the deposition of PGs in FF occurs before the deposition of collagen [30]. Therefore, the 3 patterns observed on Al-B staining and immunostaining were defined as 3 stages: stage I [A_A(Al-B) >75%], stage II [75% >A_A(Al-B) >25%], and stage III [A_A(Al-B) <25%]. Stage II was observed in all 16 patients. Stages I and III were not identified in 2 and 3 patients, respectively (Table 2).

3.3. Stage-specific characterization of MMP-2 and TIMP-2 expression

The distribution of MMP-2 and TIMP-2 expression was characterized for each stage. In stage I, both MMP-2 and TIMP-2 were expressed in the fibroblasts and the overlying epithelium (Fig. 5A-C). In the later stages, the expression of TIMP-2 was attenuated both in the fibroblasts and the overlying epithelium. In contrast, the expression of MMP-2 persisted in the fibroblasts, although it was not observed in the overlying epithelium (Fig. 5D-F).

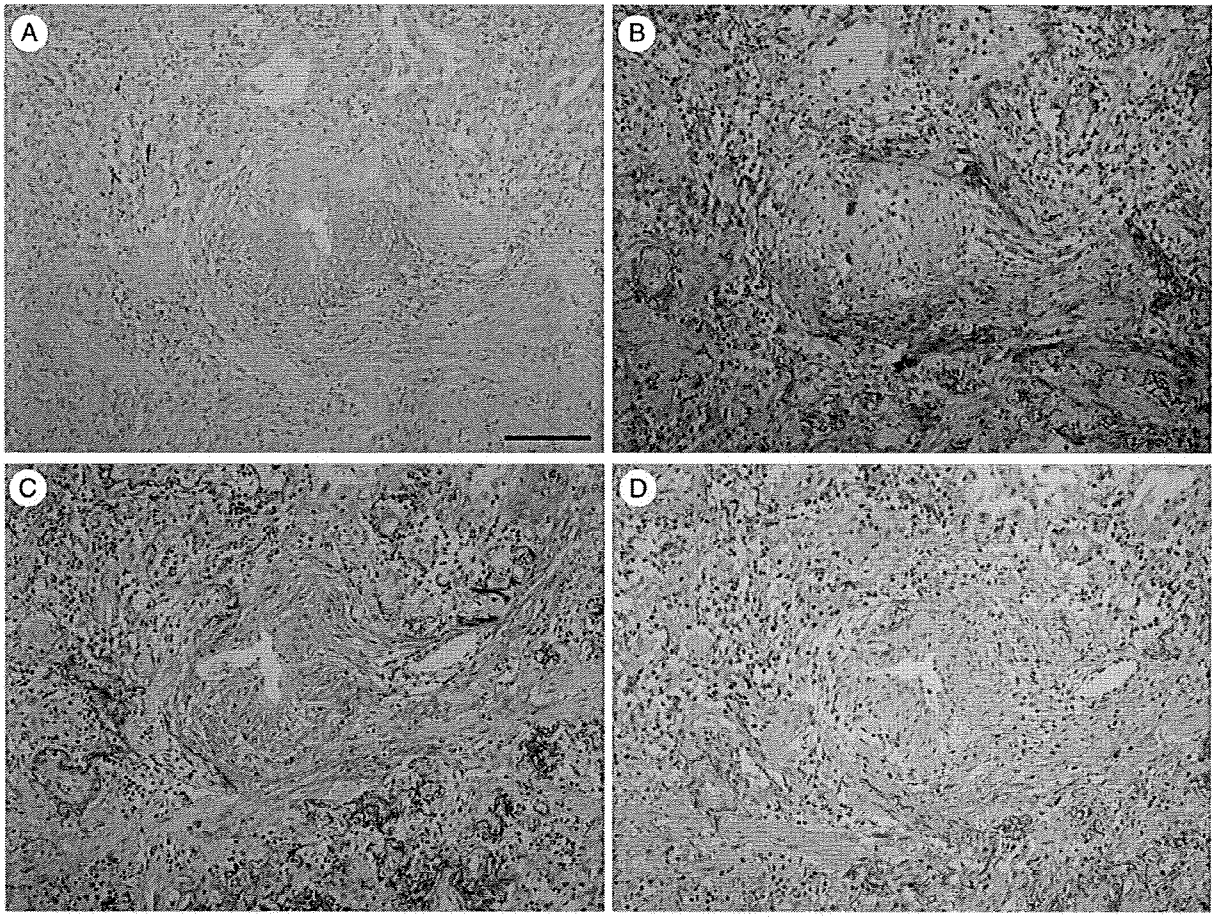

Fig. 2 A mixed pattern of fibroblastic foci. The second set of serial sections shows that Al-B stains in the inner side of a fibroblastic focus (A), whereas the expression of type I collagen (B) and ICTP (C) is observed in the peripheral side where Al-B staining is not detected. D, The expression of PICP is only observed in the inner side of fibroblasts in the focus. Hematoxylin (A-D) and Resorcin-fuchsin (B-D) for counterstain. Scale bar represents 100 μm.

3.4. Stage-specific characterization of capillary angiogenesis and lymphangiogenesis

The distribution of blood and lymphatic vessels in the 3 stages was investigated. $CD34^+$ capillaries were absent in stage I (Fig. 6A, B); a small number of capillaries were observed in the $ICTP^+$ lesions in stage II (Fig. 6C, D); and the capillaries were found to be widely distributed in stage III (Fig. 6E, F). Morphometric analysis demonstrated that a significant correlation exists between A_A(ICTP) and N_A(cap) ($r = 0.488$, $P < .001$) (Fig. 6G). On the other hand, $D2\text{-}40^+$ lymphatic vessels were undetectable in the FF across all 3 stages (Fig. 6B, D, F).

4. Discussion

In the present study, 3 different patterns of Al-B staining and ICTP immunostaining was observed in FF—Al-B–dominant, ICTP-dominant, and mixed. The results obtained indicate that the deposition of GAGs and collagen in FF may be regulated via 2 distinct processes. Bensadoun et al [30] have reported that the deposition of $Al\text{-}B^+$ GAGs in lesions associated with IPF, bronchiolitis obliterans organizing pneumonia, and diffuse alveolar damage (DAD) is dependant on the deposition of versican, which is a type of PG. Although collagen deposition was barely detected in lesions with versican deposition, type I procollagen was expressed in the myofibroblasts present in the lesions; thus, they hypothesized that this PG may influence early repair processes in IPF before collagen deposition. Our findings were consistent with those of Bensadoun et al. Moreover, a morphological analysis of the mixed pattern demonstrated that collagen deposition was dominant in the region outside the FF where GAG degradation was observed. A significant negative correlation was observed between the $Al\text{-}B^+$ and $ICTP^+$ area densities in the FF. These results suggest that the deposition of collagen begins after the degradation of GAGs. Based on these histopathologic characteristics, 3 stages were defined in FF, namely, stage I, characterized by GAG-dominant deposition; stage II, characterized by mixed

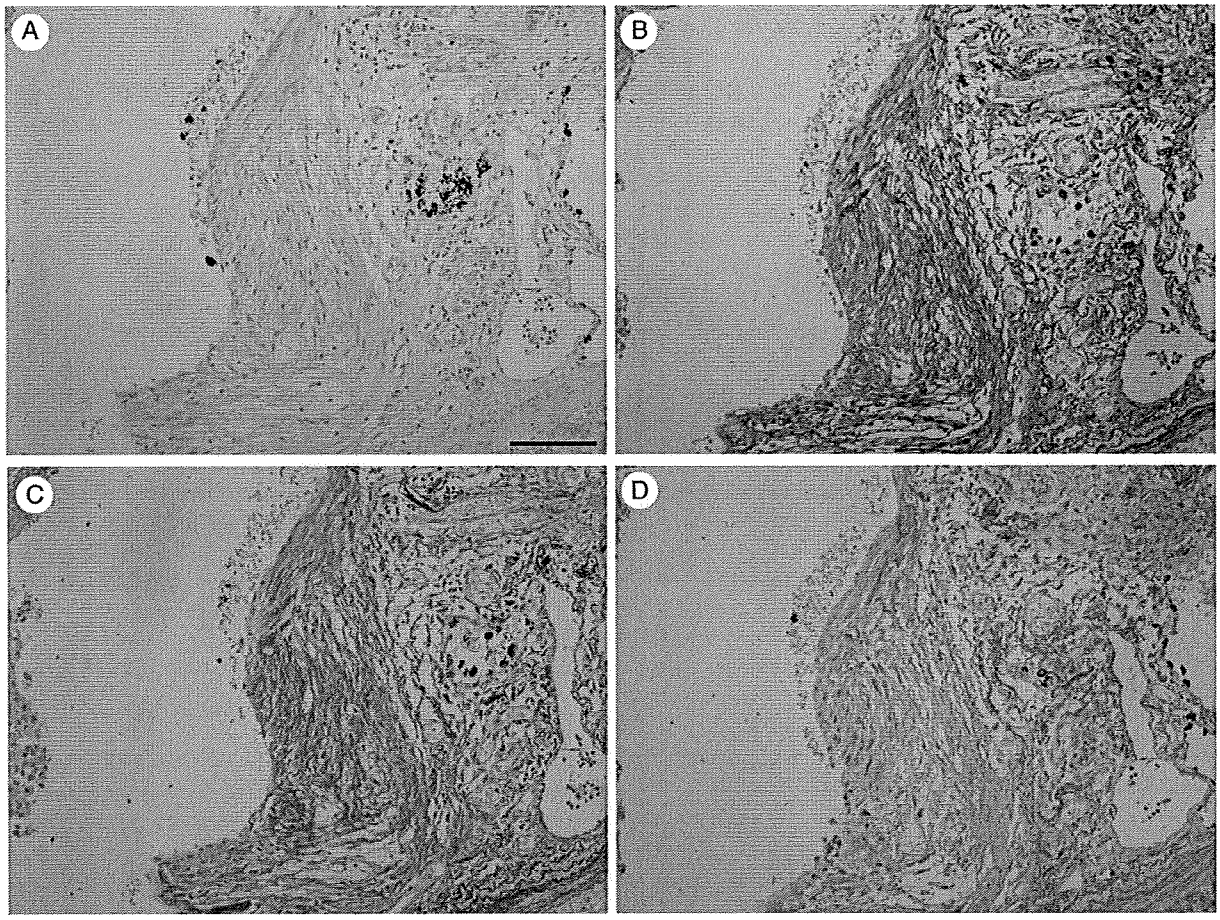

Fig. 3 A collagen-dominant pattern of fibroblastic foci. The third set of serial sections shows that Al-B weakly stains in a fibroblastic focus (A), whereas the expression of type I collagen (B) and ICTP (C) is observed in the whole ECM of the focus. D, The expression of PICP is observed in fibroblasts of the focus. Hematoxylin (A-D) and Resorcin-fuchsin (B-D) for counterstain. Scale bar represents 100 μm.

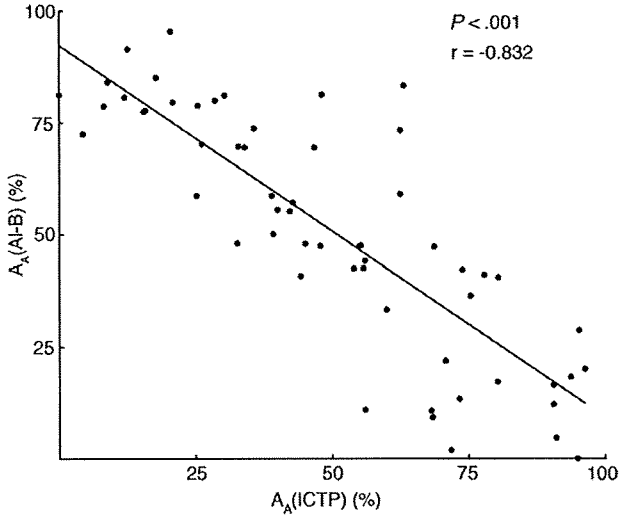

Fig. 4 A negative correlation between Al-B$^+$ and ICTP$^+$ area densities in fibroblastic foci. Morphometric analysis demonstrates that there is a significantly inverse correlation between A_A(Al-B) and A_A(ICTP).

deposition of GAGs and collagen; and stage III, characterized by collagen-dominant deposition. All 3 stages were detectable in the specimens of almost all patients, suggesting that this pathologic staging represents the fibrogenic processes occurring in FF but not the differences in the etiology and outcome of IPF.

It was noted that, in stage I, type I collagen was barely deposited in the ECM, although PICP was already expressed in the fibroblasts. Typically, procollagen is secreted from the fibroblasts and cleaved by proteases to form collagen fibrils, the basic structural units of a collagen fiber/tendon. This is followed by the cross-linking of collagen [37]. There is limited information regarding the factors regulating the release of procollagen by fibroblasts. In our study, morphological observation showed that the expression of ICTP was distributed in the lesions where GAGs were degraded. We speculate that an inhibitory factor may be actively involved in inhibiting the secretion of procollagen from fibroblasts in stage I. For example, PGs may prevent fibroblasts from releasing procollagen via integrin signals.

Table 2 The profile of the patients with IPF

Patient	Age/sex	Total/FF (stage I/II/III)[a]
1	58/F	7 (1/3/3)
2	69/M	23 (10/9/4)
3	78/M	9 (2/5/2)
4	58/F	4 (0/3/1)
5	67/F	24 (5/12/7)
6	58/F	10 (6/3/1)
7	64/M	8 (2/4/2)
8	63/F	6 (1/2/3)
9	66/M	10 (1/4/5)
10	67/M	7 (0/4/3)
11	50/M	4 (2/1/1)
12	76/M	7 (5/2/0)
13	67/F	14 (5/6/4)
14	63/M	5 (1/4/0)
15	57/M	9 (3/4/1)
16	52/M	2 (0/2/0)

[a] The number of FF in each stage.

There has been increasing evidence in support of MMP-2 and TIMP-2 involvement in matrix turnover in cases of pulmonary fibrosis [16-23]. It has been shown that TIMP-2 is expressed in the overlying epithelium and fibroblasts of FF in IPF [16,17,22]. The coexpression of TIMP-2 and Ki-67 (a marker for cell proliferation) was observed in the fibroblasts of FF [18]. The findings of these reports suggest that TIMP-2 is involved in the stable deposition of collagen and fibronectin, as well as the regulation of fibroblast proliferation. It has been reported that MMP-2 is also expressed in the fibroblasts of FF [22]. Batimastat—a synthetic inhibitor of MMPs—mainly down-regulates MMP-2 and MMP-9 in mice with bleomycin-induced pulmonary fibrosis; moreover, the down-regulation of MMPs was associated with a decrease in the proliferation of fibroblasts. Furthermore, this down-regulation was associated with a decrease in collagen deposition [38]. In these reports, it was speculated that the inconsistent expression of MMP-2 may contribute to the degradation of the epithelial basement membrane, thus facilitating the migration of fibroblasts into the FF.

In the present study, the expression of MMP-2 and TIMP-2 in FF during stage I was observed in overlying epithelial cells and in the fibroblasts of the FF. In the later stages, however, the expression of TIMP-2 was attenuated in all cells of the FF. In contrast, the expression of MMP-2 was

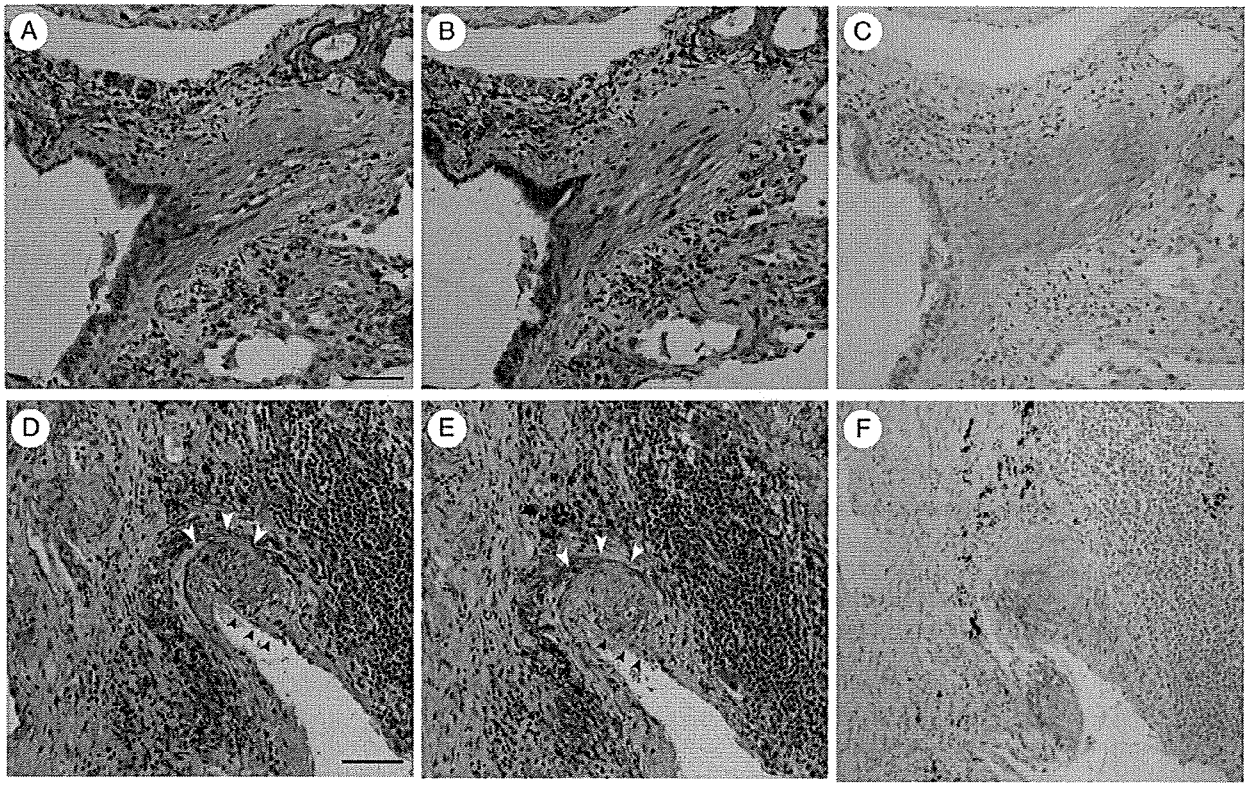

Fig. 5 Characterization of MMP-2 and TIMP-2 expression in the 3 stages. The upper set of serial sections (A-C) shows that the expression of MMP-2 (A) and TIMP-2 (B) is observed in fibroblasts and the overlying epithelium in stage I. The lower set of serial sections (D-F) shows that the expression of MMP-2 (D) persists in fibroblasts in the later stage (white arrowheads), although it is not observed in the overlying epithelium (black arrowheads). (E) In contrast, the expression of TIMP-2 is attenuated both in fibroblasts (white arrowheads) and the overlying epithelium (black arrowheads). C and F, Al-B staining. Hematoxylin (A-F) and Resorcin-fuchsin (A, B, D, and F) for counterstain. Scale bar represents 100 μm.

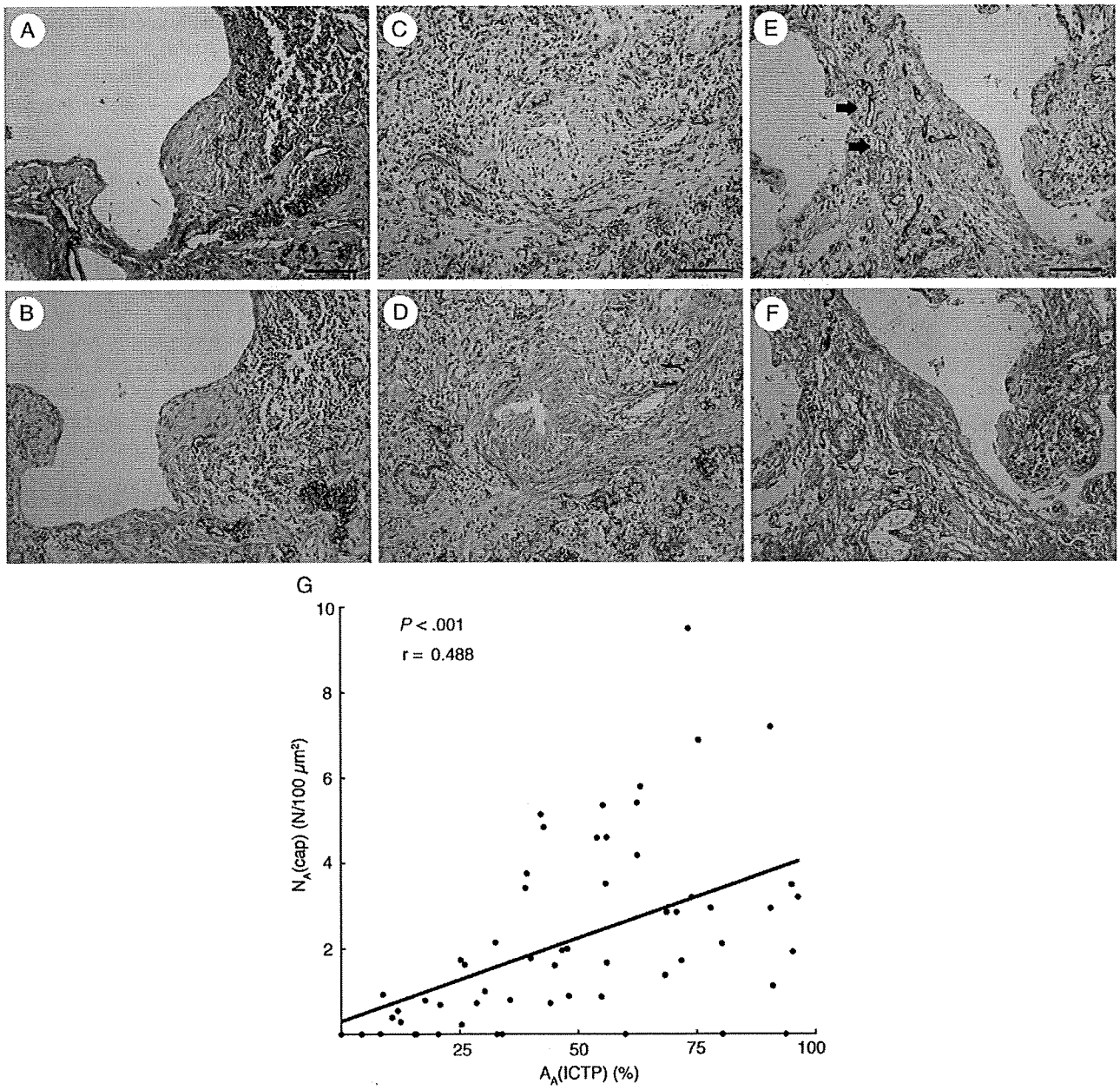

Fig. 6 Characterization of capillary angiogenesis and lymphangiogenesis in the 3 stages. A and B, A set of serial sections shows that $CD34^+$ capillaries (red in A) are not observed in a $ICTP^{weak}$ fibroblastic focus (B) in stage I. C and D, Another set of serial sections shows that in stage II, several $CD34^+$ capillaries (red in C) are observed in the peripheral $ICTP^+$ lesions of a fibroblastic focus (D), although undetectable in the inner $ICTP^{weak}$ side. E and F, The other of serial sections shows that $CD34^+$ capillaries (red in E) are widely distributed in a $ICTP^+$ fibroblastic focus (F) in stage III. $D2\text{-}40^+$ lymphatic vessels (brown in A, C, and E) are not found in FF across all 3 stages, although they can be detected outside FF (arrows in E). (G) Morphometric analysis demonstrates that there is a significant correlation between A_A(ICTP) and N_A(cap). Hematoxylin and Resorcin-Fuchsin for counterstain. Scale bar represents 100 μm.

found to persist in the fibroblasts of the FF, where GAGs were characteristically degraded. MMP-2 has been shown to regulate the degradation of PGs [39,40]. Our results suggest that TIMP-2 contributes to the stabilization of GAG deposition in the earlier stage (stage I), whereas MMP-2 may participate in PG degradation in the later stages (stages II and III). It was noted that apart from the overlying epithelium, the periphery of the FF also showed degradation of GAGs in stage II. These findings imply that the overlying epithelial cells strongly regulate GAG turnover.

The relationship between capillary angiogenesis and pulmonary fibrosis is interesting [24-29]. In some reports,

capillaries in FF have been shown to be barely detectable in IPF [28,29]. In contrast, Masson's body—an organized fibrotic lesion that is manifested in cryptogenic organizing pneumonia—was observed to be highly capillarized [27]. Because the fibrosis of Masson's body is dissoluble, it has been hypothesized that the absence of capillaries in FF may correlate to the poor prognosis of IPF. In the present study, the capillaries were observed in the later stages, an observation inconsistent with the previous findings. A positive correlation was observed between A_A(ICTP) and N_A(cap), and MMP-2 has been reported to induce capillary angiogenesis [41-43]. In cases of IPF, MMP-2 in fibroblasts may facilitate capillary angiogenesis in the later stages. It is still unknown whether delayed capillary formation in FF is involved in the pathogenesis of IPF.

In contrast to capillary angiogenesis, lymphangiogenesis was barely detected in FF throughout the 3 stages. Lymphangiogenesis has been reported in various pathophysiologic conditions such as tumor metastasis and inflammatory conditions; however, there is limited information regarding lymphangiogenesis in the case of pulmonary fibrosis [44-46]. In wound healing, lymphangiogenesis occurs after angiogenesis through sprouting of preexisting lymphatics, and the resultant lymphatic system is transient [46]. However, in a prolonged healing process such as that associated with chronic skin ulcer, lymphangiogenesis occurs to a lesser extent than in the case of the normal healing process [46]. It has been hypothesized that newly formed lymphatics play a pivotal role in the later stages of wound healing. Pulmonary fibrosis is believed to be a consequence of aberrant healing after a lung injury [1]. It would be interesting to determine whether the absence of lymphangiogenesis in FF is associated with the indissoluble deposition of collagen in FF.

We have previously reported that, in idiopathic DAD, lymphangiogenesis was observed in the intra-alveolar fibrotic lesions during the proliferative stage, in which capillary angiogenesis was absent [31]. The intra-alveolar fibrotic lesions in DAD are similar to the FF in IPF in terms of irreversible fibroproliferation, but the results of the histopathologic characterization of the 2 types of angiogenesis in DAD were in contrast to those of the present study. The reason why capillary angiogenesis and lymphangiogenesis show contrasting features between the 2 conditions is unclear. These results indicate that the dominance of neither capillary angiogenesis nor lymphangiogenesis is related to the irreparability of pulmonary fibrosis.

In conclusion, this is the first report to demonstrate that the factors involved in tissue remodeling in IPF, including MMP-2 and TIMP-2, and the 2 types of angiogenesis show different histopathologic characteristics among the 3 stages. The findings of the present study provide new insight into the roles of these factors in tissue remodeling. The pathologic stages elucidated in this study will facilitate further investigations regarding the fibrogenic processes in IPF.

Acknowledgments

The authors thank Dr Keiichi Saito for their excellent helps.

References

[1] Selman M, King TE, Pardo A, American Thoracic Society, European Respiratory Society, American College of Chest Physicians. Idiopathic pulmonary fibrosis: prevailing and evolving hypotheses about its pathogenesis and implications for therapy. Ann Intern Med 2001;134: 136-51.

[2] Katzenstein AL, Myers JL. Idiopathic pulmonary fibrosis: clinical relevance of pathologic classification. Am J Respir Crit Care Med 1998;157:1301-15.

[3] Basset F, Ferrans VJ, Soler P, et al. Intraluminal fibrosis in interstitial lung disorders. Am J Pathol 1986;122:443-61.

[4] Katzenstein AL, Myers JL, Prophet WD, et al. Bronchiolitis obliterans and usual interstitial pneumonia. A comparative clinicopathologic study. Am J Surg Pathol 1986;10:373-81.

[5] Myers JL, Katzenstein AL. Epithelial necrosis and alveolar collapse in the pathogenesis of usual interstitial pneumonia. Chest 1988;94: 1309-11.

[6] Kuhn 3rd C, Boldt J, King Jr TE, et al. An immunohistochemical study of architectural remodeling and connective tissue synthesis in pulmonary fibrosis. Am Rev Respir Dis 1989;140:1693-703.

[7] Kuhn C, McDonald JA. The roles of the myofibroblast in idiopathic pulmonary fibrosis. Ultrastructural and immunohistochemical features of sites of active extracellular matrix synthesis. Am J Pathol 1991;138: 1257-65.

[8] King Jr TE, Schwarz MI, Brown K, et al. Idiopathic pulmonary fibrosis: relationship between histopathologic features and mortality. Am J Respir Crit Care Med 2001;164:1025-32.

[9] Nicholson AG, Fulford LG, Colby TV, et al. The relationship between individual histologic features and disease progression in idiopathic pulmonary fibrosis. Am J Respir Crit Care Med 2002;166:173-7.

[10] Hanak V, Ryu JH, de Carvalho E, et al. Profusion of fibroblast foci in patients with idiopathic pulmonary fibrosis does not predict outcome. Respir Med 2008;102:852-6.

[11] Selman M, Montaño M, Ramos C, et al. Concentration, biosynthesis and degradation of collagen in idiopathic pulmonary fibrosis. Thorax 1986;41:355-9.

[12] Lammi L, Ryhänen L, Lakari E, et al. Type III and type I procollagen markers in fibrosing alveolitis. Am J Respir Crit Care Med 1999;159: 818-23.

[13] Kaarteenaho-Wiik R, Lammi L, Lakari E, et al. Localization of precursor proteins and mRNA of type I and III collagens in usual interstitial pneumonia and sarcoidosis. J Mol Histol 2005;36:437-46.

[14] Fukuda Y, Basset F, Ferrans VJ, et al. Significance of early intra-alveolar fibrotic lesions and integrin expression in lung biopsy specimens from patients with idiopathic pulmonary fibrosis. Hum Pathol 1995;26:53-61.

[15] Motomiya M, Arai H, Sato H, et al. Increase of dermatan sulfate in a case of pulmonary fibrosis. Tohoku J Exp Med 1975;115:361-5.

[16] Hayashi T, Stetler-Stevenson WG, Fleming MV, et al. Immunohistochemical study of metalloproteinases and their tissue inhibitors in the lungs of patients with diffuse alveolar damage and idiopathic pulmonary fibrosis. Am J Pathol 1996;149:1241-56.

[17] Fukuda Y, Ishizaki M, Kudoh S, et al. Localization of matrix metalloprotcinases-1, -2, and -9 and tissue inhibitor of metalloproteinase-2 in interstitial lung diseases. Lab Invest 1998;78:687-98.

[18] Selman M, Ruiz V, Cabrera S, et al. TIMP-1, -2, -3, and -4 in idiopathic pulmonary fibrosis. A prevailing nondegradative lung microenvironment? Am J Physiol Lung Cell Mol Physiol 2000;279: L562-74.

[19] Suga M, Iyonaga K, Okamoto T, et al. Characteristic elevation of matrix metalloproteinase activity in idiopathic interstitial pneumonias. Am J Respir Crit Care Med 2000;162:1949-56.
[20] Lemjabbar H, Gosset P, Lechapt-Zalcman E, et al. Overexpression of alveolar macrophage gelatinase B (MMP-9) in patients with idiopathic pulmonary fibrosis: effects of steroid and immunosuppressive treatment. Am J Respir Cell Mol Biol 1999;20:903-13.
[21] Ramos C, Montaño M, García-Alvarez J, et al. Fibroblasts from idiopathic pulmonary fibrosis and normal lungs differ in growth rate, apoptosis, and tissue inhibitor of metalloproteinases expression. Am J Respir Cell Mol Biol 2001;24:591-8.
[22] Kelly MM, Leigh R, Gilpin SE, et al. Cell-specific gene expression in patients with usual interstitial pneumonia. Am J Respir Crit Care Med 2006;174:557-65.
[23] Oggionni T, Morbini P, Inghilleri S, et al. Time course of matrix metalloproteases and tissue inhibitors in bleomycin-induced pulmonary fibrosis. Eur J Histochem 2006;50:317-25.
[24] Keane MP, Arenberg DA, Lynch III JP, et al. The CXC chemokines, IL-8 and IP-10, regulate angiogenic activity in idiopathic pulmonary fibrosis. J Immunol 1997;159:1437-43.
[25] Keane MP, Belperio JA, Burdick MD, et al. ENA-78 is an important angiogenic factor in idiopathic pulmonary fibrosis. Am J Respir Crit Care Med 2001;164:2239-42.
[26] Lappi-Blanco E, Soini Y, Kinnula V, et al. VEGF and bFGF are highly expressed in intraluminal fibromyxoid lesions in bronchiolitis obliterans organizing pneumonia. J Pathol 2002;196:220-7.
[27] Lappi-Blanco E, Kaarteenaho-Wiik R, Soini Y, et al. Intraluminal fibromyxoid lesions in bronchiolitis obliterans organizing pneumonia are highly capillarized. Hum Pathol 1999;30:1192-6.
[28] Renzoni EA, Walsh DA, Salmon M, et al. Interstitial vascularity in fibrosing alveolitis. Am J Respir Crit Care Med 2003;167:438-43.
[29] Cosgrove GP, Brown KK, Schiemann WP, et al. Pigment epithelium-derived factor in idiopathic pulmonary fibrosis: a role in aberrant angiogenesis. Am J Respir Crit Care Med 2004;170:242-51.
[30] Bensadoun ES, Burke AK, Hogg JC, et al. Proteoglycan deposition in pulmonary fibrosis. Am J Respir Crit Care Med 1996; 154:1819-28.
[31] Yamashita M, Iwama N, Date F, et al. Characterization of lymphangiogenesis in various stages of idiopathic diffuse alveolar damage. Hum Pathol 2009 [Electronic publication ahead of print].
[32] Matsui K, Nagy-Bojarsky K, Laakkonen P, et al. Lymphatic microvessels in the rat remnant kidney model of renal fibrosis: aminopeptidase p and podoplanin are discriminatory markers for endothelial cells of blood and lymphatic vessels. J Am Soc Nephrol 2003;14:1981-9.
[33] Ishikawa Y, Akishima-Fukasawa Y, Ito K, et al. Lymphangiogenesis in myocardial remodeling after infarction. Histopathology 2007;51: 345-53.
[34] American Thoracic Society. Idiopathic pulmonary fibrosis: diagnosis and treatment. International consensus statement. American Thoracic Society (ATS), and the European Respiratory Society (ERS). Am J Respir Crit Care Med 2000;161:646-64.
[35] Risteli J, Elomaa I, Niemi S, et al. Radioimmunoassay for the pyridinoline cross-linked carboxy-terminal telopeptide of type I collagen: a new serum marker of bone collagen degradation. Clin Chem 1993;39:635-40.
[36] Weibel ER. Stereological methods. Volume 1. Practical methods for biological morphometry. Orlando (Fla): Academic Press; 1979. p. 26-39.
[37] Kumar V, Abbas AK, Fausto N. Robbins and Cotran. Pathologic basis of disease. 7th ed. Philadelphia, Pennsylvania: Elsevier Saunders; 2005. p. 103-6.
[38] Corbel M, Caulet-Maugendre S, Germain N, et al. Inhibition of bleomycin-induced pulmonary fibrosis in mice by the matrix metalloproteinase inhibitor batimastat. J Pathol 2001;193:538-45.
[39] Zuo J, Ferguson TA, Hernandez YJ, et al. Neuronal matrix metalloproteinase-2 degrades and inactivates a neurite-inhibiting chondroitin sulfate proteoglycan. J Neurosci 1998;18:5203-11.
[40] Passi A, Negrini D, Albertini R, et al. The sensitivity of versican from rabbit lung to gelatinase A (MMP-2) and B (MMP-9) and its involvement in the development of hydraulic lung edema. FEBS Lett 1999;456:93-6.
[41] Rivilis I, Milkiewicz M, Boyd P, et al. Differential involvement of MMP-2 and VEGF during muscle stretch- versus shear stress-induced angiogenesis. Am J Physiol Heart Circ Physiol 2002;283:H1430-8.
[42] Ohno-Matsui K, Uetama T, Yoshida T, et al. Reduced retinal angiogenesis in MMP-2-deficient mice. Invest Ophthalmol Vis Sci 2003;44:5370-5.
[43] Zheng H, Takahashi H, Murai Y, et al. Expressions of MMP-2, MMP-9 and VEGF are closely linked to growth, invasion, metastasis and angiogenesis of gastric carcinoma. Anticancer Res 2006;26:3579-83.
[44] Skobe M, Hawighorst T, Jackson DG, et al. Induction of tumor lymphangiogenesis by VEGF-C promotes breast cancer metastasis. Nat Med 2001;7:192-8.
[45] Baluk P, Tammela T, Ator E, et al. Pathogenesis of persistent lymphatic vessel hyperplasia in chronic airway inflammation. J Clin Invest 2005; 115:247-57.
[46] Paavonen K, Puolakkainen P, Jussila L, et al. Vascular endothelial growth factor receptor-3 in lymphangiogenesis in wound healing. Am J Pathol 2000;156:1499-504.

厚生労働科学研究費補助金

医療機器開発推進研究事業

ナノバブルと超音波を用いた
高周波超音波三次元画像診断・分子導入システムの開発

平成20年度　総括・分担研究報告書

研究代表者　小玉　哲也

平成21（2009）年　4月

目　　次

総　括　研　究　報　告

厚生労働科学研究費補助金（医療機器開発推進研究事業）
平成２０年度　総括研究報告書

ナノバブルと超音波を用いた高周波超音波三次元画像診断・分子デリバリーシステムの開発

課題番号：H19-ナノ-一般-010

主任研究者　小玉　哲也　東北大学大学院医工学研究科

研究要旨：リンパ節転移マウスモデルの作製に成功し，超音波画像解析装置と大型計算機と連動させることで，三次元血管構築画像を抽出するという独自の画像解析システムを開発した．一方，超音波とナノバブルを使用した分子導入法で，固形腫瘍への薬剤導入をおこない，本分子導入法の抗腫瘍効果を実証した．長期的に発現可能な長期発現性プラスミドDNAの開発に成功し，本分子導入法で問題とされる一過性の遺伝子発現性を克服することができた．走査型電子顕微鏡観察から，本研究で開発したナノバブルは，内部にガスと液体が封入された音響性ナノバブルであることを実証した．効果的な気泡崩壊を誘導するために，気泡を分散させた水中での超音波の透過，反射等の計算が可能な，線形解析および非線形解析を進めた．以上の成果より，平成20年10月より「頭頸部癌症例の不顕性リンパ節転移検出」に関し，東北大学病院の倫理委員会の承認を得て臨床試験を開始し，三次元の血管抽出データからリンパ節転移の早期診断の有効性を検討している．

分担研究者

小野栄夫	東北大学大学院医学系研究科・教授
福本　学	東北大学加齢医学研究所・教授
森　士朗	東北大学病院・講師
松村保広	国立がんセンター東病院・部長
藤川重雄	北海道大学大学院工学研究科・教授

A．研究目的

本研究では，超音波造影性薬剤封入型ナノバブルと超音波を用いて，がんの微小血管に特徴的な血管周囲へのバブルの溢出・貯留効果をバブルの軌跡として捉えて三次元画像を構築し，その構築画像の特徴からがんの診断をおこない，同時に輝度の集積部への超音波照射によりバブルを破裂させ，封入された抗腫瘍分子をがん組織に導入可能な高周波超音波三次元画像診断・分子導入システムを開発する．

まず，臨床試験導入用リンパ節転移モデル・肝転移モデルを作製し，三次元画像診断法を開発する．本分子導入法の抗腫瘍効果を実証するために，抗腫瘍分子を固形腫瘍に導入し，その治療効果を実証した．一過性の遺伝子発現性特性を改善するために長期発現性プラスミドDNAを開発する．高い分子導入効率を目指すために音響理論から，超音波場でのナノバブルの動特性を解明した．ナノバブルの形態は走査型電子顕微鏡で観察した．平成20年10月より「頭頸部癌症例の不顕性リンパ節転移検出」に関し，東北大学病院の倫理委員会の承認を得て臨床試験を開始し，前臨床試験の成果を実証している．

B．研究方法

1. 音響性ナノバブルの作製

平成19年度に開発した作製法にしたがい，内部にガスと液体が封入された音響性ナノバブルを作製し，走査型電子顕微鏡で形態を観察する．

2. 臨床試験導入用動物実験モデルの作製

2.1. 肝転移モデル

マウス脾臓にルシフェラーゼ発現性腫瘍 (EMT6-Luc, Colon26-Luc)を移植し，1週間後に脾臓を摘出する．

2.2. 所属リンパ節転移モデル

MRL/MpJ-*lpr/lpr*マウスのリンパ節にルシフェラーゼ発現性腫瘍MRL-KM-Lucを移植する．

3. がんの早期診断法の開発：マウス尾静脈にナノバブルを注射し，腫瘍内血管を流れるバブルを高周波超音波で探知し，大型計算機で輝度情報を処理する.つぎに，がんに特徴的な形状や血管密度を評価し，がんの早期診断を開発する．

4. 長期発現性プラスミドDNAの開発

ルシフェラーゼ遺伝子を組入れた長期発現性プラスミドを合成する．

5. 分子導入法システムの開発

腫瘍血管内を流れるバブルの輝度値をトリガー信号にして超音波照射が可能な超音波システムを開発する．

6. 分子導入機序の解明

殻付微細気泡の形状，径分布等の基本物理特性を明らかにし，これらの特性と吸収との関係を解明した．また，分子動力学シミュレーションにより，バブルバブル崩壊で発生する衝撃圧の作用にともなう細胞膜変形を解析した．

（倫理面への配慮）

動物実験は，各施設の動物倫理委員会の了承を得て実施する． 臨床試験は，東北大学大学院医学系研究科第1倫理委員会および第2倫理委員会で了承を得る．

C．研究結果および考察

1. 音響性ナノバブルの形態学観察

平均直径が200nm音響性リポゾームを走査型電子顕微鏡で観察し，ガスと液体が封入されていることを明らかにした．本実験で開発に成功したナノバブルはドラッグキャリア型音響性ナノバブルであることを示した．

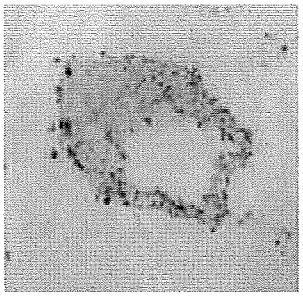

図1. ナノバブル.走査型顕微鏡観察で内部に液体とガスが封入されていることを確認.

2. 臨床試験導入用動物実験モデルの作製

2.1. 肝転移モデル

腫瘍細胞を脾臓に移植し, 門脈経由で形成された肝転移モデル系の確立した.転移の移動をインドシアニン・グリーン (ICG)で観察した.

2.2. 所属リンパ節転移モデル

MRL/MpJ-*lpr/lpr*マウスの鼠径リンパ節に腫瘍を移植し, 腋窩リンパ節に転移可能なリンパ節転移モデルの開発に成功した.

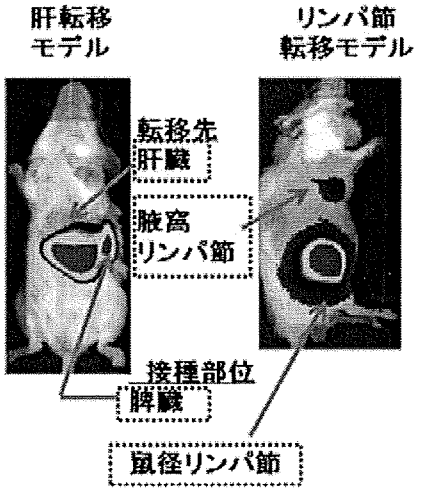

図2. 臨床試験導入用動物実験モデルの作製

3. がんの早期診断法の開発

腫瘍血管内を流れるバブルの輝度情報から血管を抽出することができた.

4. 分子導入法システムの評価

低出力超音波 (US) とマイクロバブル(MB) を使用した分子導入法による抗腫瘍効果を検討した. HT29-Luc ヒト結腸癌ルシフェラーゼ発現性細胞で作製したマウス固形腫瘍の治療効果を生体発光イメージング法で解析した. 図3 は, 細胞移植後11日目での

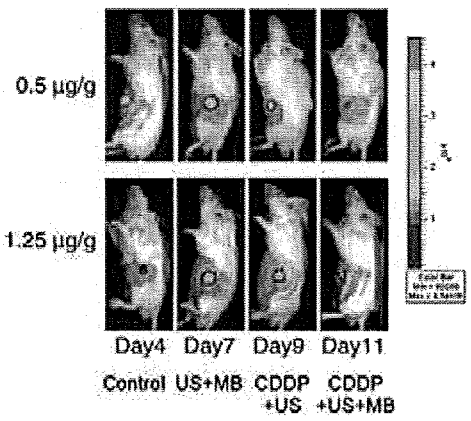

図3. 生体発光イメージング法.

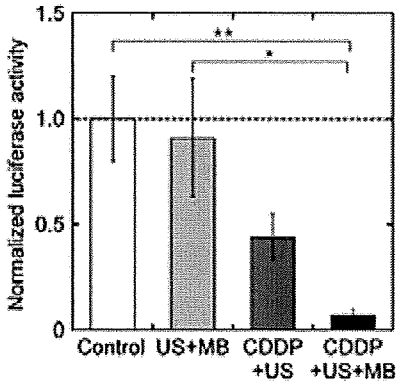

図4. 抗腫瘍効果の検討. US : 超音波, MB : ナノマイクロバブル, CDDP : シスプラチン

抗腫瘍効果を，コントロール群で無次元化したものである．USとMBを組合せることで，外来分子を効率よく腫瘍細胞内に導入し，抗腫瘍効果を得ることができる(図4)．将来的には局所療法として有効な膀胱がん，肝がん，卵巣がんに応用可能であると考えられる．

5．長期発現性プラスミドDNAの開発
ルシフェラーゼ発現
ルシフェラーゼ遺伝子を組入れた長期発現性プラスミドDNAを作製した．マウス骨格筋に導入し，発現時間を100日以上持続することを生体発光イメージング法で確認した．

6．分子導入機序の解明
超音波とナノ・マイクロバブル(NMB)を併用した分子導入法では，超音波の作用で崩壊するキャビテーション気泡からの衝撃波が，細胞膜の構造変化を誘導し，外来分子が細胞内に導入されるものと考えられる．本研究では，細胞膜を脂質二重膜としてモデル化し，この膜に対する衝撃波の入斜角度が脂質二重膜の構造変化に与える影響を調べた．脂質の頭部と尾部の横変位は，衝撃波が入射する二重層の上流層側内で観察され，下流層側には観察されないこと，この結果，斜め衝撃波の脂質に対する運動量の垂直成分のみが，下流層側の脂質の構造変化に関与することが示された(図5)．また，本研究では，ナノスケールの殻付微細気泡を通過した超音波は特定の周波数において減衰をともなうことを明らかにした．

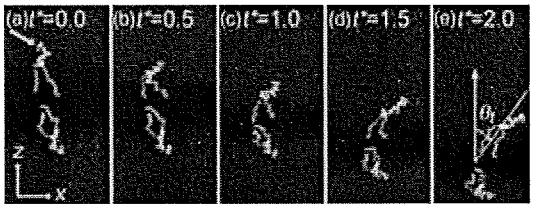

図5．斜め衝撃波の作用にともなう脂質分子の構造変化．二重膜を構成する上流側の一つの分子を黄色で描写．赤は脂質二重膜構造の外側に配置された水分子を示す．

図6．頭頸部癌症例の不顕性リンパ節転移検出

7．臨床試験
平成20年10月より「頭頸部癌症例の不顕性リンパ節転移検出」に関し，東北大学病院の倫理委員会の承認を得て臨床試験を開始した．三次元の血管抽出データからリンパ節転移の早期診断を実施し，前臨床試験の結果の有効性を評価している(図6)．

D．結論

ドラッグキャリアと音響性の機能をもつ音響性ナノバブルを開発することに成功した．臨床導入用転移マウスモデルの作製に成功した．このマウスを使用した前臨床試験で平成20年10月より「頭頸部癌症例の不顕性リンパ節転移検出」に関し，東北大学病院の倫理委員会の承認を得て臨床試験を開始し，三次元の血管抽出データからリンパ節転移の早期診断の実用性の検討を開始した．臨床試験の成果を精査し，早期がん診断法の開発を目指す．また，基礎実験として，理論解析および理論解析を実施し，ナノバブルと超音波を使用した分子導入機序を明らかにした．

F．健康危険情報

特になし

G．研究発表

別紙参照

H．知的財産権の出願・登録状況

1．熊谷啓之，小玉哲也．医薬組成物．特願 2008-208041．2008年8月12日

研究成果の刊行に関する一覧表

雑誌

発表者氏名	論文タイトル名	発表誌名	巻号	ページ	出版年
Suzuki R, Oda Y, Utoguchi N, Namai E, Taira Y, Okada N, Kadowaki N, Kodama T, Tachibana K, Maruyama K.	A novel strategy utilizing ultrasound for antigen delivery in dendritic cell-based cancer immunotherapy.	Journal of Controlled Release.	133	198-205	2009
Kodama T, Tomita Y, Watanabe Y, Koshiyama K, Yano T, Fujikawa S.	Cavitation bubbles mediated molecular delivery during sonoporation.	Journal of Biomechanical Science and Engineering	4	124-140	2009
Koshiyama K, Kodama T, Yano T, Fujikawa S.	Molecular dynamics simulation of structural changes of lipid bilayers induced by shock waves: effects of incident angles.	Biochimica et Biophysica Acta (BBA) - Biomembranes.	1778(6)	1423-1428	2008
Watanabe Y, Aoi A, Horie S, Tomita N, Mori S, Morikawa H, Matsumura Y, Vassaux G, Kodama T.	Low-intensity ultrasound and microbubbles enhance the antitumor effect of cisplatin.	Cancer Science.	99(12)	2525-2531	2008

国際会議での発表

発表者氏名	論文タイトル名	学会・研究会名	巻号	ページ	開催日	開催地
Ishii K, Funaki Y, Kikuch Y, Yamazaki H, Matsuyama S, Terakawa A, Fujiwara M, Iwata R, Kodama T, Watanabe Y, Tanizaki N, Amano D, Yamaguchi T.	FDG imaging of 1mm tumor with an ultras resolution animal PET.	The Fifth IEEE International Symposium on Biomedical Imaging (ISBI'08)			May 14-17, 2008.	Paris, France
Tomita Y, Inaba T, Uchikoshi R, Kodama T.	Peeling off effect and damage pit formation by ultrasonic cavitation.	The International Conference on Hydraulic Machinery and Equipments			October 16-17, 2008.	Timisoara, Romania,
Horie S, Watanabe Y, hen R, Tomita N, Oosawa F, Fujisawa S, Ono M, Fukumoto M, Mori S, Matsumura Y, Kodama T.	Bladder cancer therapy using nanobubbles and two different intensities of ultrasound.	The 2008 Nanomedicine Conference.	Program	p5.	19-24 September 2008.	Hotel Eden Roc, Sant Feliu de Guixols, Spain.
Chen R, Chiba M, Watanabe Y, Horie S, Tomita N, Fukumoto M, Nori S, Kodama T.	Local gene delivery system of nano/microbubbles-enhanced ultrasound aimed for treatment of gingival tumor.	2008 International Conference on Frontiers of Dental and Craniofacial Research.	Program pp	96-97.	November 1-3, 2008.	Beijing International Convention Center (BICC), Beijing, China,